How Often Does It Rain?

YING SUN* AND SUSAN SOLOMON

NOAA/Aeronomy Laboratory, Boulder, Colorado

AIGUO DAI

National Center for Atmospheric Research,+ Boulder, Colorado

ROBERT W. PORTMANN

NOAA/Aeronomy Laboratory, Boulder, Colorado

(Manuscript received 20 January 2005, in final form 1 September 2005)

ABSTRACT

Daily precipitation data from worldwide stations and gridded analyses and from 18 coupled global climate models are used to evaluate the models' performance in simulating the precipitation frequency, intensity, and the number of rainy days contributing to most (i.e., 67%) of the annual precipitation total. Although the models examined here are able to simulate the land precipitation amount well, most of them are unable to reproduce the spatial patterns of the precipitation frequency and intensity. For light precipitation (1–10 mm day^{-1}), most models overestimate the frequency but produce patterns of the intensity that are in broad agreement with observations. In contrast, for heavy precipitation (>10 mm day^{-1}), most models considerably underestimate the intensity but simulate the frequency relatively well. The average number of rainy days contributing to most of the annual precipitation is a simple index that captures the combined effects of precipitation frequency and intensity on the water supply. The different measures of precipitation characteristics examined in this paper reveal region-to-region differences in the observations and models of relevance for climate variability, water resources, and climate change.

1. Introduction

The distribution of worldwide precipitation has been the focus of many studies (e.g., Legates and Willmott 1990; Xie and Arkin 1997; Huffman et al. 1997; Adler et al. 2003), but other characteristics relevant to climate research, such as the frequency of occurrence, intensity, and the contribution of heavy rainfall to total amount, are also attracting increasing attention. For example, Trenberth et al. (2003) argued that in a warmer climate, where the amount of atmospheric moisture is expected to rise faster than the total precipitation amount, increases in precipitation intensity must be offset by decreases in precipitation frequency. However, these characteristics have been subject to limited analysis using observations and models. Evaluating the global distribution of these parameters from observations and testing how well climate models deal with these characteristics of precipitation is the focus of this paper.

Using global weather reports, Dai (2001) first documented the spatial and seasonal variations in the frequency of various types of precipitation (drizzle, nondrizzle, showery and nonshowery, and snow) on a global scale. Higgins et al. (1996) examined the climatology of precipitation frequency over the United States using hourly rain gauge data. Petty (1995) analyzed shipboard weather reports and showed seasonal maps of precipitation frequencies at various intensities over the

* Current affiliation: National Climate Center, China Meteorological Administration, Beijing, China.

+ The National Center for Atmospheric Research is sponsored by the National Science Foundation.

Corresponding author address: Dr. Ying Sun, National Climate Center, China Meteorological Administration, 46 Zhongguancun Nandajie, Beijing 100081, China.
E-mail: yingsun75@yahoo.com

oceans. From a climate change viewpoint, Karl and Knight (1998) suggested that in the United States an increase in the number of days with precipitation has occurred since 1910 for all categories of precipitation amounts, and they also suggested an increase in the intensity of extremely heavy precipitation events. Groisman et al. (2005) further pointed out that systematic changes (mostly increases) in heavy daily precipitation have occurred during the past 100 yr in various regions of the world (including the contiguous United States). Projections from climate models have suggested that there will be increased precipitation intensity (albeit with regional variations) in future climates with increased greenhouse gases, not only in earlier studies but also using improved and more sophisticated models (e.g., Meehl et al. 2000). These studies indicate important qualitative consistency between the models and observations regarding changes in precipitation intensity.

It is important to examine not only the qualitative behavior but also how well models simulate precipitation characteristics for the current climate. Many models produce reasonable patterns of precipitation amounts, but this could result from incorrect combinations of precipitation frequency and intensity, as shown by earlier analyses (Chen et al. 1996; Dai et al. 1999). It is generally thought that a common problem in many climate models is that precipitation occurs too frequently at reduced intensity (Dai and Trenberth 2004). Here we systematically evaluate the performance of current global coupled climate models in simulating daily precipitation amount, frequency, intensity, and the number of the locally heavy precipitation days. We compare model simulations of the precipitation frequency and intensity to available observations, explicitly separating light (1–10 mm day^{-1}) and heavy (>10 mm day^{-1}) precipitation to provide more detailed information. We show that the characteristics of these two different classes of precipitation in the models are quite different, which has important implications for interpretating the challenges posed to climate models.

We also consider the number of rainy days over which most of the total precipitation in a given location falls. A cutoff of 67% (or about two-thirds) of the precipitation is used in this study. Tests showed that the results are similar for other chosen cutoff values. Figure 1 shows the distribution of the average number of days in a year that contribute 67% of the precipitation based upon the Global Historical Climatology Network [GHCN; (National Climatic Data Center) (NCDC) 2002]. Many interesting features are revealed by this index, including the very limited number of days (<25) that typically dominate the annual precipitation in Australia, North Africa, eastern South America, and some parts of China and North America. Even in places where rainfall is known to be frequent such as the Northwest United States and much of Europe, it is interesting to note that most of the total annual precipitation typically occurs in fewer than 80 days. As will be discussed further below, these results underscore the episodic nature of the events that dominate the total precipitation in many different regions. Simulating these episodic events is thus an important challenge for numerical models.

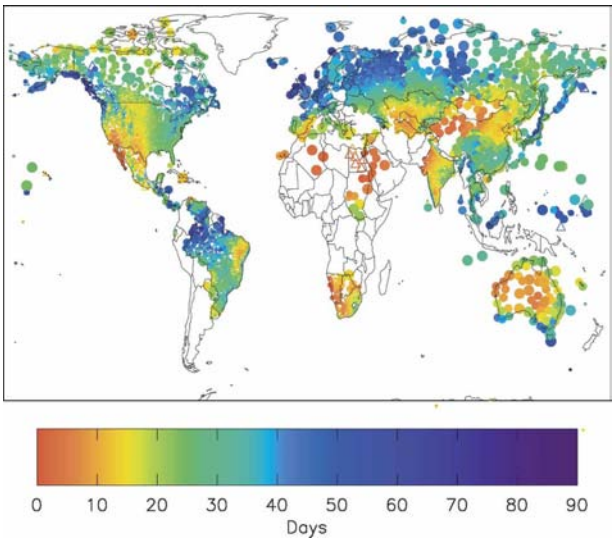

FIG. 1. Long-term mean number of rainy days contributing 67% of the annual precipitation computed using the station daily precipitation data during 1840–2001 (with varying lengths for different stations). Stations with <5 yr records (only years with >300 day records are used here) are shown as open triangles.

The scope of this paper is limited to precipitation intensity, frequency, and amount and does not represent a complete evaluation of model performance. It should be noted that this limited analysis must be complemented by studies examining many other aspects of model performance, including temperature distribution, ENSO, radiative fluxes, etc.

The structure of the paper is as follows. In section 2, the precipitation data and climate models are described, while section 3 compares the total rainfall amount from observations and 18 climate models. The precipitation frequency and intensity are compared in sections 4 and 5, respectively. In section 6, the number of days typically contributing 67% of the annual precipitation from observations and models is discussed. A discussion of various model convection parameterizations is given in section 7. Section 8 provides a summary of the results.

2. Data, models, and analysis methods

The observational data used in this study include the daily precipitation dataset (1840–2001) from the GHCN compiled at the NCDC (NCDC 2002), the gridded daily precipitation data (0.5° × 0.5°, 1979–2003) based on rain gauge data included in the Global Telecommunication System (GTS; P. Xie 2005, personal communication) and the monthly global precipitation dataset (2.5° × 2.5°, 1979–2002) derived from rain gauge observations and satellite estimates (Xie and Arkin 1997). The GHCN daily data are station rain gauge records of varying length (only years with >300 day records are used, and stations with <5 yr records are shown as open triangles in the figures). Data are available over most land areas, with sampling being densest over most of North America, East Asia, eastern Australia, eastern Brazil, India, South Africa, central Mexico, the southern half of the former U.S.S.R., and Europe (cf. Fig. 1). The gridded daily precipitation data were derived by Xie et al. (1996) at the National Centers for Environmental Prediction (NCEP) from GTS precipitation reports (~6000 stations) using the algorithm of Shepard (1968). In this paper, we averaged the 0.5° × 0.5° data onto 1° × 1° and 3° × 3° to compare with model outputs.

The reason to use different daily precipitation datasets is because the precipitation frequency and intensity calculated using station and gridded data could be different, as gridding averages station precipitation and thus may increase the frequency and reduce the intensity. The effect is illustrated using a 1° × 1° grid box that contains eight stations in the southeastern United States (31°–32°N, 82°–83°W). The frequency of light precipitation using the gridded data for this grid box is ~0.52, which is much higher than that (~0.1–0.2) at individual stations, while the intensity of heavy precipitation calculated using gridded values is ~11 mm day^{-1}, compared with that (22–24 mm day^{-1}) at individual stations. This kind of obvious difference resulting from the use of different observational data is further seen over some regions (e.g., in Figs. 3 and 6).

We also found that using the GTS data precipitation frequency increases with grid size as expected. However, the spatial patterns stay the same and the differences between 1° and 3° grids are relatively small compared with the differences among the models and between the observations and models. This suggests that differences in the model grids should not affect the frequency and intensity patterns significantly. In this paper, we use the results from all the original model outputs and do not interpolate them to the same resolution. This approach helps us to directly derive information from the model itself, especially for those models with a relatively high resolution.

The model-simulated daily precipitation data for current climate are extracted from the second phase of the Coupled Model Intercomparison Project (CMIP2+; Covey et al. 2003) datasets and the Intergovernmental Panel on Climate Change (IPCC) simulations for the Fourth Assessment [AR4; except for the Geophysical Fluid Dynamics Laboratory (GFDL) CM2.0 with Donner's cumulus parameterization provided to us by L. Donner 2005, personal communication]. The CMIP2+ collected the outputs from both model control runs and matching runs in which CO_2 increases at the rate of 1% yr^{-1} (Covey et al. 2003). The IPCC AR4 dataset consists of the outputs from the newest generation of coupled ocean–atmosphere general circulation models (CGCM) and has been archived at the Program for Climate Model Diagnosis and Intercomparison (PCMDI) since the end of 2004 (more information available online at http://www-pcmdi.llnl.gov/ipcc/about_ipcc.php). To explore the possible effects of model physical parameterization schemes and resolution on precipitation characteristics, the results from available old and new versions of certain models will be presented and compared. In this paper, we analyzed daily precipitation data from 7 models from their control runs in CMIP2+, and from 11 models from their twentieth-century climate simulations (20c3m) in the IPCC AR4 experiments. Table 1 summarizes the information about the models and the simulation. A summary of the precipitation parameterization schemes used in the models is also given in Table 1, which is discussed further in section 7.

In this study, precipitation is classified into two categories based on daily rates: light (1–10 mm day^{-1}) and heavy (>10 mm day^{-1}) precipitation. Because drizzle contributes little to total precipitation amounts measured by rain gauges over most areas (Dai 2001), the days with precipitation <1 mm day^{-1} were not counted. However, the recent results from Dai (2005, manuscript submitted to *J. Climate*, hereafter DAI) show that drizzle (<1 mm day^{-1}) contributes 8% to the total precipitation (for the average of 50°S–50°N) in the Tropical Rainfall Measuring Mission (TRMM) data and 12%–14% in the current climate models. Precipitation frequency was calculated by dividing the number of days with light or heavy precipitation by the number of all days, with data expressed as a percentage. The mean precipitation intensity was calculated as the mean precipitation rates over days with light or heavy precipitation.

As stated in the introduction, a simple index is introduced to evaluate model performance in reproducing

TABLE 1a. Climate models compared in this study that have participated in the IPCC AR4.

Model name	Center/country	Atmospheric resolution (lat × lon)	Cloud parameterization	Convective parameterization
CCSM3	NCAR/United States	T85 (1.4° × ~1.4°)	Prognostic cloud condensate with diagnostic cloud amount	Parameterization schemes developed by Zhang and McFarlane (1995) and Hack (1994)
CGCM3.1	CCCma/Canada	T32 (~3° × 3.75°)	Prognostic cloud evaluated through a relative humidity threshold; precipitation occurs whenever the local relative humidity is supersaturated	Moist convective adjust scheme
CNRM-CM3	CNRM/France	T63 (2.8° × ~2.8°)	Statistical cloud scheme of Ricard and Royer (1993)	Mass flux convective scheme with Kuo-type closure of Bougeault (1985)
GFDL-CM2.0	GFDL/United States	2.0° × 2.5°	Microphysics (Rotstayn et al. 2000) and macrophysics (Tiedtke 1993)	Relaxed Arakawa–Schubert (Moorthi and Suarez 1992)
GFDL-CM2.0 Donner	GFDL/United States	2.0° × 2.5°	Same as GFDL-CM2.0	Donner's cumulus convection scheme (Donner et al. 2001)
GISS-ER	GISS/United States	4° × 5°	Prognostic cloud following Sundqvist (1978) and Sundqvist et al. (1989)	Mass flux approach by Del Genio and Yao (1993)
INM-CM3.0	INM/Russia	4° × 5°	Stratiform cloud fraction calculated as linear function of relative humidity	Deep and shallow convection after Betts (1986), but with changed referenced profile for deep convection
IPSL-CM4	IPSL/France	2.5° × 3.75°	The cloud cover and in-cloud water deduced from the large-scale total water and moisture at saturation (Bony and Emmanuel 2001)	Moist convection is treated using a modified version (Grandpeix et al. 2004) of the Emanuel (1991) scheme
MIROC3.2-medres	CCSR/NIES/ FRCGC/Japan	T42 (2.8° × ~2.8°)	Prognostic total water scheme based on Le Treut and Li (1991) with the second indirect effect of aerosols based on Berry (1967)	Prognostic closure of Arakawa–Schubert based on Pan and Randall (1998) with the empirical suppression condition based on Emori et al. (2001)
MIROC3.2-hires	CCSR/NIES/ FRCGC/Japan	T106 (~1.12° × 1.125°)	Same as MIRO3.2-medres	Same as MIRO3.2-medres
PCM	NCAR/United States	T42 (2.8° × ~2.8°)	Same as CCSM3	Same as CCSM3

TABLE 1b. Same as in Table 1a, but climate models from CMIP2+.

Model name	Center/country	Atmospheric resolution (lat × lon)	Cloud parameterization	Convective parameterization
CCSM2	NCAR/USA	T42 (2.8° × ~2.8°)	Prognostic condensation-based cloud	A parameterization scheme developed by Zhang and McFarlane (1995)
CSIRO Mk2	CSIRO/Austrilia	R21 (~3.2° × 5.625°)	Prognostic relative humidity–based cloud (similar to Slingo 1987)	Moist convective adjustment scheme
ECHAM4_OPYC3	MPIfM/DKRZ/ Germany	T42 (2.8° × ~2.8°)	Large-scale rainfall calculations based on cloud water and ice contents (based on Sundqvist 1978)	Mass flux scheme (Tiedtke 1989) with modifications for penetrative convection according to Nordeng (1994)
ECHO_G	MPIfM/Germay	T30 (~3° × 3.75°)	Same as ECHAM4	Same as ECHAM4
GFDL R30	GFDL/USA	R30 (~2.2° × 3.75°)	Precipitation simulated whenever supersaturation is indicated by the prognostic equation for water vapor	Moist convective adjustment scheme (Manabe et al. 1965)
HadCM3	UKMO/UK	2.5° × 3.75°	Large-scale rainfall and snowfall calculations based on cloud water and ice contents (similar to Smith 1990)	Mass flux penetrative convection scheme (Gregory and Rowntree 1990), with the improvement by Gregory et al. (1997)
MRI	MRI/Japan	T42 (2.8° × ~2.8°)	Condensation based cloud	Arakawa-Schubert scheme based on Randall and Pan (1993) with some modifications

how frequently heavy precipitation occurs that dominates the total annual accumulation. This variable, denoted as N_{67}, is the average number of days that make up most (selected cutoff of 67%) of the total annual precipitation. The calculation procedure is as follows. For each year we sort the daily precipitation data from the heaviest to the lightest. We then count the number of the heaviest precipitation days (N_{67}) that are required to accumulate 67% of the annual precipitation. Then the climatological mean $\overline{N}_{67}$ and standard deviation D_{67} of N_{67} are calculated. Note that the standard deviation shown here has been normalized (i.e., divided) by $\overline{N}_{67}$ and thus is unitless. Different from the conventional precipitation frequency and intensity, the number of days contributing 67% of the annual precipitation provides a complementary and simple way to quantify how many precipitation events typically dominate the local precipitation budget over different regions, since it makes no assumption of any particular intensity (e.g., 1–10 versus >10 mm day^{-1}, etc.).

3. Precipitation climatology

Various studies have investigated the capability of climate models to reproduce mean precipitation patterns (e.g., Roeckner et al. 1996; Yukimoto et al. 2001; Gordon et al. 2002; Delworth et al. 2002; Covey et al. 2003; Min et al. 2005; Delworth et al. 2006; Schmidt et al. 2006). In this section, simple comparisons between observations and models are shown to give a broad picture of mean precipitation amount before discussions of precipitation intensity and frequency. Since observations of daily precipitation are available only over land, we will focus on land precipitation. In this paper, we present observations for June–August (JJA) for the purposes of illustration but discuss results for the December–February (DJF) season as well.

Figure 2 shows the observed (Xie and Arkin 1997) and model-simulated mean precipitation amounts for boreal summer JJA. Generally, all the models capture many of the large-scale features well. Significant discrepancies are seen over the central United States (too wet in many models), northern South America (too dry), and many mountainous regions, such as the Tibetan Plateau, the Rocky Mountains and the Andes. For JJA, all the models are able to broadly reproduce the monsoon precipitation over India, eastern and Southeastern Asia, and Africa, but with some wet biases over the Indo-China Peninsula for most of the models. There are dry biases over India and East China for the Commonwealth Scientific and Industrial Research Organisation (CSIRO), the Meteorological Research Institute (MRI), the fourth-generation Max Planck Institute (MPI), model (ECHAM4)_OPYC3,

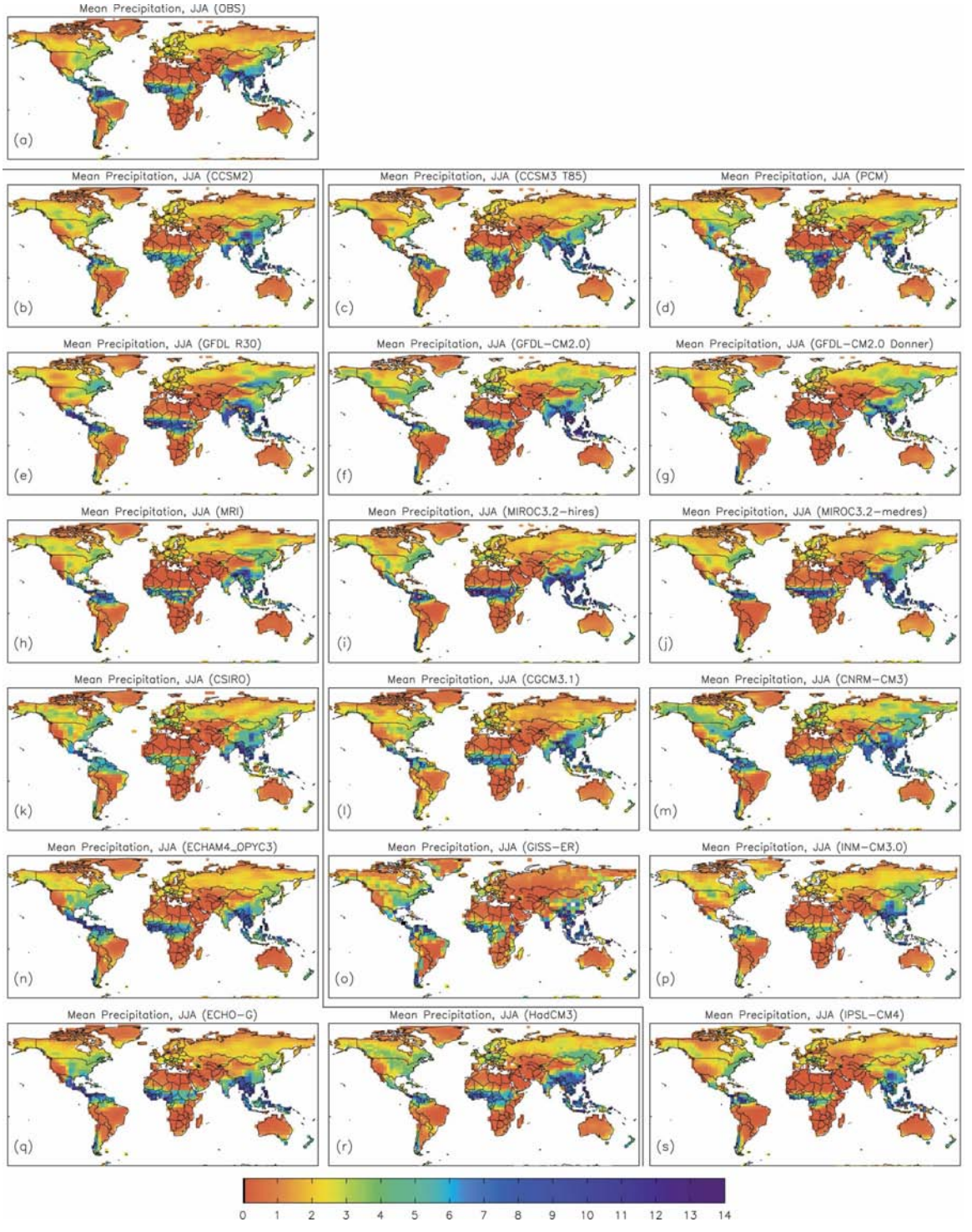

FIG. 2. Mean precipitation amount (mm day^{-1}) for JJA from (a) observations (Xie and Arkin 1997) and 18 models: (b) CCSM2, (c) CCSM3, (d) PCM, (e) GFDL-R30, (f) GFDL-CM2.0, (g) GFDL-CM2.0 Donner, (h) MRI, (i) MIROC3.2-hires, (j) MIOC3.2-medres, (k) CSIRO, (l) CGCM3.1, (m) CNRM-CM3, (n) ECHAM4_OPYC3, (o) GISS-ER, (p) INM-CM3.0, (q) ECHO-G, (r) HadCM3, and (s) IPSL-CM4. (top) Indicates the results of observations, (left) the results from CMIP2+ models, and (right) the results from the IPCC models.

T30 version of ECHAM4 and the global version of the Hamburg Ocean Primitive Equation Model (HOPE) (ECHO-G), version 3.1 of the CGCM (CGCM3.1), the Goddard Institute for Space Studies (GISS-ER), version 3.0 of the Institut National de Métrologie (INM) Coupled Model (CM3.0), and version 4 of the L'Institut Pierre-Simon Laplace (IPSL) Coupled Model (CM4) as well as dry biases over tropical Africa for CCSM2, CSIRO, GISS-ER, INM-CM3.0 and IPSL-CM4. Most of the models produce excessive rainfall over the eastern part of North America, and dry biases also exist in the southeast United States in the CCSM2 and GFDL R30 models.

Compared with CCSM2 (at T42 resolution), CCSM3 (at T85 resolution) shows improved ability to reproduce precipitation over the mountainous regions. The GFDL-CM2.0 is a new version completely different from GFDL-R30. The former displays a more realistic distribution over Asia but overestimates precipitation over North America. The GFDL-CM2.0 with Donner's cumulus parameterization produced an obvious difference from the original model over the United States and East Asia, and underestimates the precipitation over these two regions. The major difference between version 3 of the Model for Interdisciplinary Research on Climate (MIROC3) high- and medium-resolution models is seen over the mountainous regions. The high-resolution version produces more reasonable precipitation patterns over the Tibetan Plateau than the medium-resolution model but overestimates the precipitation over costal regions of East China. These comparisons illustrate that the simulation of precipitation is affected by many factors, in particular the precipitation parameterization scheme and model resolution.

In boreal winter (not shown), the comparisons are comparable, with models generally simulating the observed precipitation patterns well. However, wet biases in the midlatitudes of the winter hemisphere are a common problem in CMIP AOGCMs (Lambert and Boer 2001).

4. Precipitation frequency

a. Light precipitation

Figure 3 shows the geographical distribution of observed and simulated mean frequency for light precipitation in boreal summer (JJA). An obvious difference is seen between Figs. 3a and 3c. For most land areas with frequent precipitation, frequency calculated with gridded data (Figs. 3b,c) is higher than that calculated with station data, and there is no prominent difference between the patterns of GTS 1° and 3°, which is consistent with our analyses in section 2. In the northern high latitudes, light precipitation occurs frequently: ~20%–30% [for (observations) OBS-GHCN, and ~40%–50% for OBS-GTS] of the days over Canada and most of Eurasia (Fig. 3a). In the northern midlatitudes, light precipitation occurs less frequently in the United States (~10% for OBS-GHCN, ~20%–30% for OBS-GTS) than in the Asian monsoon regions (20%–30% for OBS-GHCN, and ~40%–50% for OBS-GTS). In the subtropical divergence regions, such as northern and southern Africa and the Middle East, it rains less than a few percent of the days. And in most tropical regions, such as the Amazon, tropical Africa, and Southeast Asia, it rains very frequently (more than 30% from GTS). But in most of South American and Australia, the precipitation frequency is relatively low in JJA, generally less than a few percent (Fig. 3a).

Most of the models considerably overestimate the JJA frequency of light precipitation in the Northern Hemisphere (Fig. 3). This is especially true over Canada, eastern North America, Europe, and the Asian monsoon regions. In the Southern Hemisphere, most of the models reproduce the relatively low frequency in Australia and southern Brazil, but overestimate the frequency over northern South America. The GFDL-R30 and MIROC3 high resolution (hires) and medium resolution (medres) appear to produce the most realistic patterns of light precipitation frequency.

For two versions of CCSM, some improvements are seen in CCSM3, including a smaller frequency of light precipitation over the United States and central Europe. This could be due to changes of physical processes, as well as different resolutions of the two versions. For the GFDL model series, it is obvious that light precipitation frequency is overestimated in GFDL-CM2.0. When Donner's cumulus scheme was used, a more realistic pattern is seen over the United States in the model, but no obvious improvement is found over other regions. Two versions of MIROC3.2 produce very similar and reasonable distributions of light precipitation frequency, which suggests that physical processes are more important in simulating precipitation characteristics than resolution for this particular model. More discussion will be presented in section 7.

Comparisons between the simulated and observed precipitation frequency in boreal winter (not shown) are very similar to those in JJA. Most models overestimate the frequency of light precipitation, even in Australia where the models' results are in good agreement with the observations for JJA (Fig. 3).

b. Heavy precipitation

The observed and simulated frequencies for heavy precipitation (>10 mm day^{-1}) in JJA are shown in Fig.

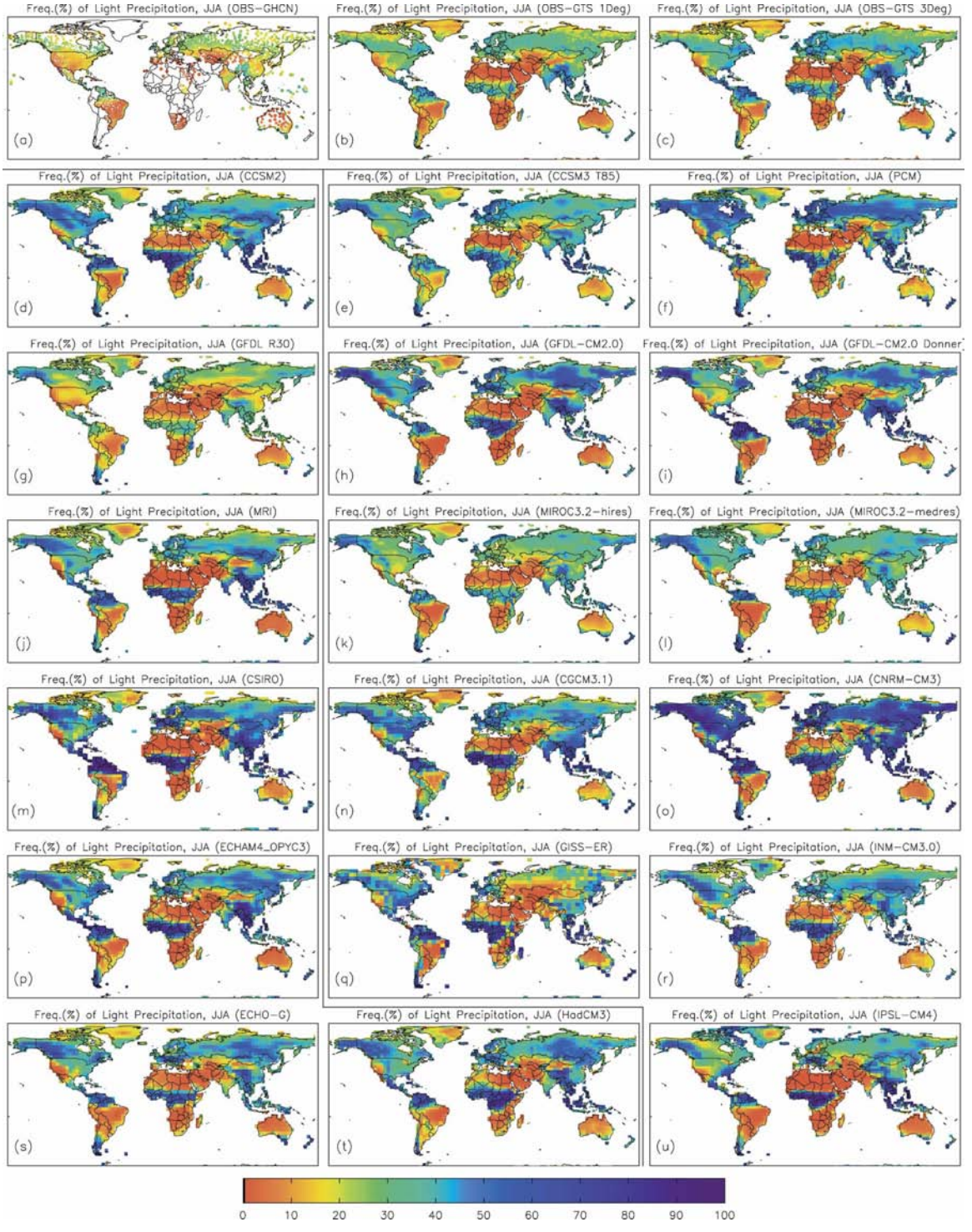

FIG. 3. Mean JJA precipitation frequency (%) for light precipitation (1–10 mm day^{-1}) from (a) station observations from GHCN (open triangles represent stations with records less than 5 yr), (b) gridded GTS observations on a 1° grid and (c) 3° grid and models: (d) CCSM2, (e) CCSM3, (f) PCM, (g) GFDL-R30, (h) GFDL-CM2.0, (i) GFDL-CM2.0 Donner, (j) MRI, (k) MIROC3.2-hires, (l) MIOC3.2-medres, (m) CSIRO, (n) CGCM3.1, (o) CNRM-CM3, (p) ECHAM4_OPYC3, (q) GISS-ER, (r) INM-CM3.0, (s) ECHO-G, (t) HadCM3, and (u) IPSL-CM4. (top) Indicates the results of observation, (left) the results from CMIP2+ models, and (right) the results from the IPCC models.

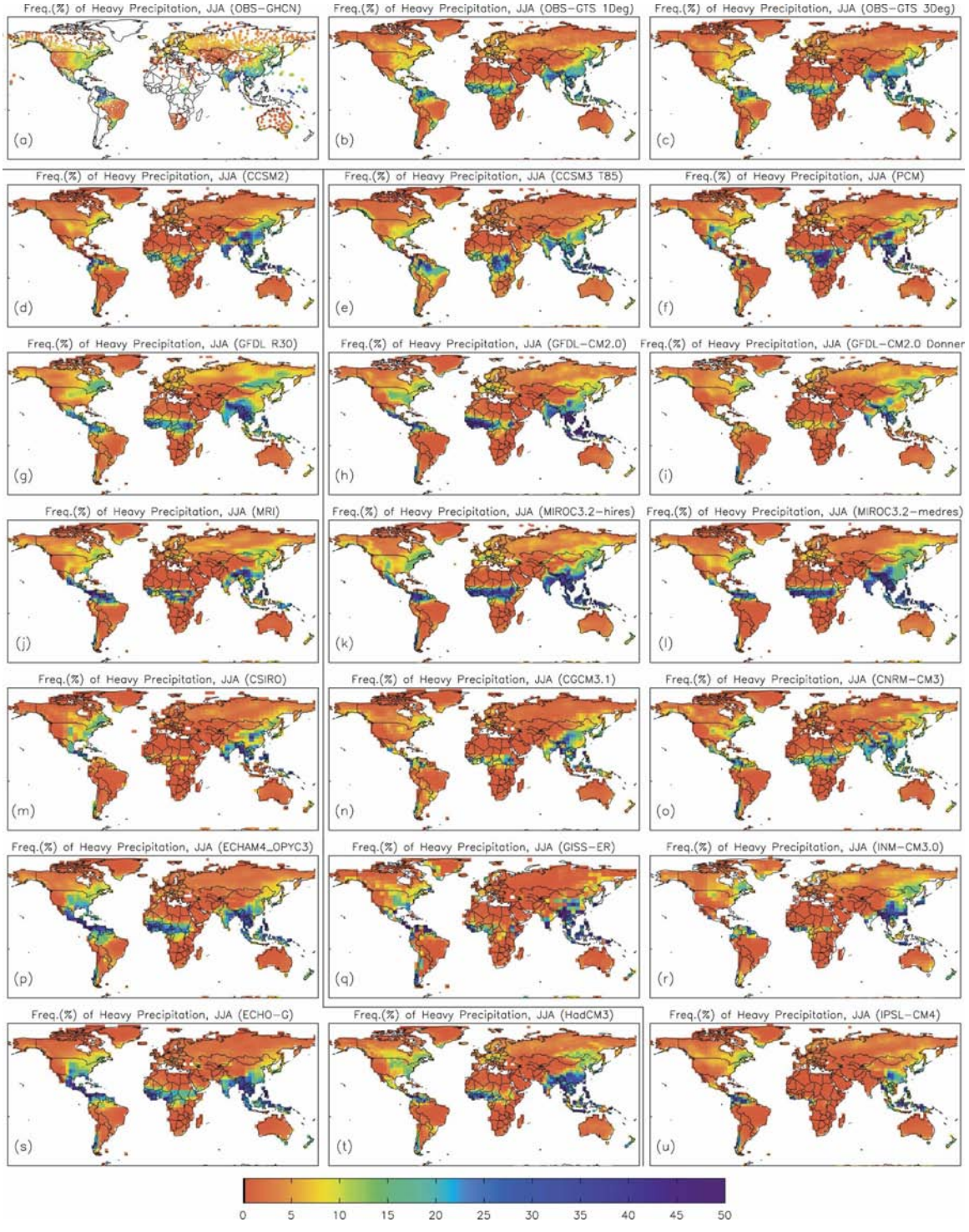

FIG. 4. Same as in Fig. 3, but for the frequency (%) of heavy precipitation (>10 mm day^{-1}).

4. As we discussed in section 2, the frequency of heavy precipitation calculated with station and gridded data only show relatively small differences (lower in the station data). As expected, heavy precipitation occurs more frequently at low latitudes than high latitudes (Figs. 4a–c). During JJA, heavy rainfall over Southeastern Asia occurs about 20%–40% of the days. In the eastern United States and eastern China, the frequency of heavy rainfall is about 15%, which is much higher than the typical values of about ~5% over the northern

high latitudes. In dry regions, such as northern and southern Africa, the Middle East, and most of Australia, heavy precipitation occurs rarely (less than a few percent), if at all (Figs. 4a–c).

Most of the models simulate the heavy precipitation frequency better than the light precipitation frequency, and they generally reproduce the large-scale pattern. Heavy precipitation frequencies in eastern North America, the Asian monsoon regions, and tropical South America are broadly reproduced (Fig. 4), although most of the models overestimate the frequency of heavy precipitation in southeastern Asia and underestimate the frequency in the northern high latitudes. These results suggest that these climate models have too many days with light precipitation, but perform rather well in simulating the heavy precipitation frequency.

For different versions of CCSM, again, over the mountainous regions, CCSM3 reproduces the heavy precipitation frequency more realistically than CCSM2. GFDL-CM2.0 simulates the frequency of heavy precipitation better than GFDL-R30 over eastern North America, India, and East Asia. For two versions of MIROC3.2, the high-resolution model simulated a higher frequency of heavy precipitation over the western United States and eastern China than the medium-resolution model. The high frequency of heavy precipitation explains why there is more total precipitation over eastern China and the western United States in the high-resolution model than that in the medium-resolution model (cf. Fig. 2). Iorio et al. (2004) showed that in one GCM, with increased spatial resolution, the simulated statistics of daily precipitation amounts improve substantially because of better representation of strong daily precipitation events through the model's large-scale precipitation mechanism. They also showed that replacing the convection parameterizations with an embedded cloud-system-resolving model radically changes the model's simulated statistics of daily precipitation amounts. However, a fuller understanding of why the change in resolution causes higher frequencies of heavy precipitation is needed.

5. Precipitation intensity

a. Light precipitation

Figure 5 shows the observed and simulated precipitation intensities for light precipitation (1–10 mm day^{-1}) in JJA. The distributions from station (Fig. 5a) and gridded data (Figs. 5b,c) do not show large differences. The mean intensity is about 3–5 mm day^{-1} in the northern mid- and high latitudes, with relatively high intensity in eastern North America and Southeast Asia (Figs. 5a–c). In dry regions, such as northern and southern Africa, the Middle East, and northern Australia, the precipitation intensity is only a few millimeters per day. Note that there are several black triangles in the observations (OBS-GHCN) shown in Fig. 5a for northern Africa (Egypt), which indicates that light precipitation has not been observed. However, this may be due to limited precipitation data there, in addition to desert conditions.

Some models, such as GFDL R30, GFDL-CM2.0 Donner, MRI, GISS-ER, and version 3 of the Hadley Centre Coupled Model (HadCM3), underestimate the intensity of light precipitation over most land areas. Most current models considerably overestimate the intensity over southern Asia, northern South America, and central Africa (Fig. 5). Over northern high latitudes, Australia, and Brazil, all the models (except for ECHAM4_OPYC3) underestimate the intensity of light precipitation. The biases in the light precipitation intensity are, however, less severe than in the light precipitation frequency.

If we look at different versions of individual models, CCSM3 displays a better simulation over the United States than CCSM2, but no obvious improvement is seen over most other regions. Compared with GFDL-R30 and GFDL-CM2.0 Donner, GFDL-CM2.0's simulation is closer to observations although GFDL-CM2.0 overestimates the light precipitation intensity over the eastern United States, tropical Africa, and most Asian regions. Very similar patterns are seen in MIROC3.2 high and medium resolution (i.e., "hires" and "medres," respectively). There is no obvious influence from model resolution on the simulation of light precipitation intensity.

Seasonal variations of the precipitation intensity are quite large. In DJF, the regions with a high intensity (>3 mm day^{-1}) of light precipitation are mainly located in the Southern Hemisphere (not shown). The models generally capture this seasonal change and reproduce the high intensity in the Amazon and South Africa. However, the simulated DJF light precipitation intensity over Australia is too low in all the models compared with the observations.

b. Heavy precipitation

Figure 6 compares the observed and simulated mean intensity of heavy (>10 mm day^{-1}) precipitation for JJA. In the observations, the intensity calculated with station data (Fig. 6a) is much stronger than that calculated with grid data (Figs. 6b,c). Heavy precipitation is smoothed during area averaging as we noted in section 2. In the central and eastern United States, the Asian monsoon regions, northern South America, and tropi-

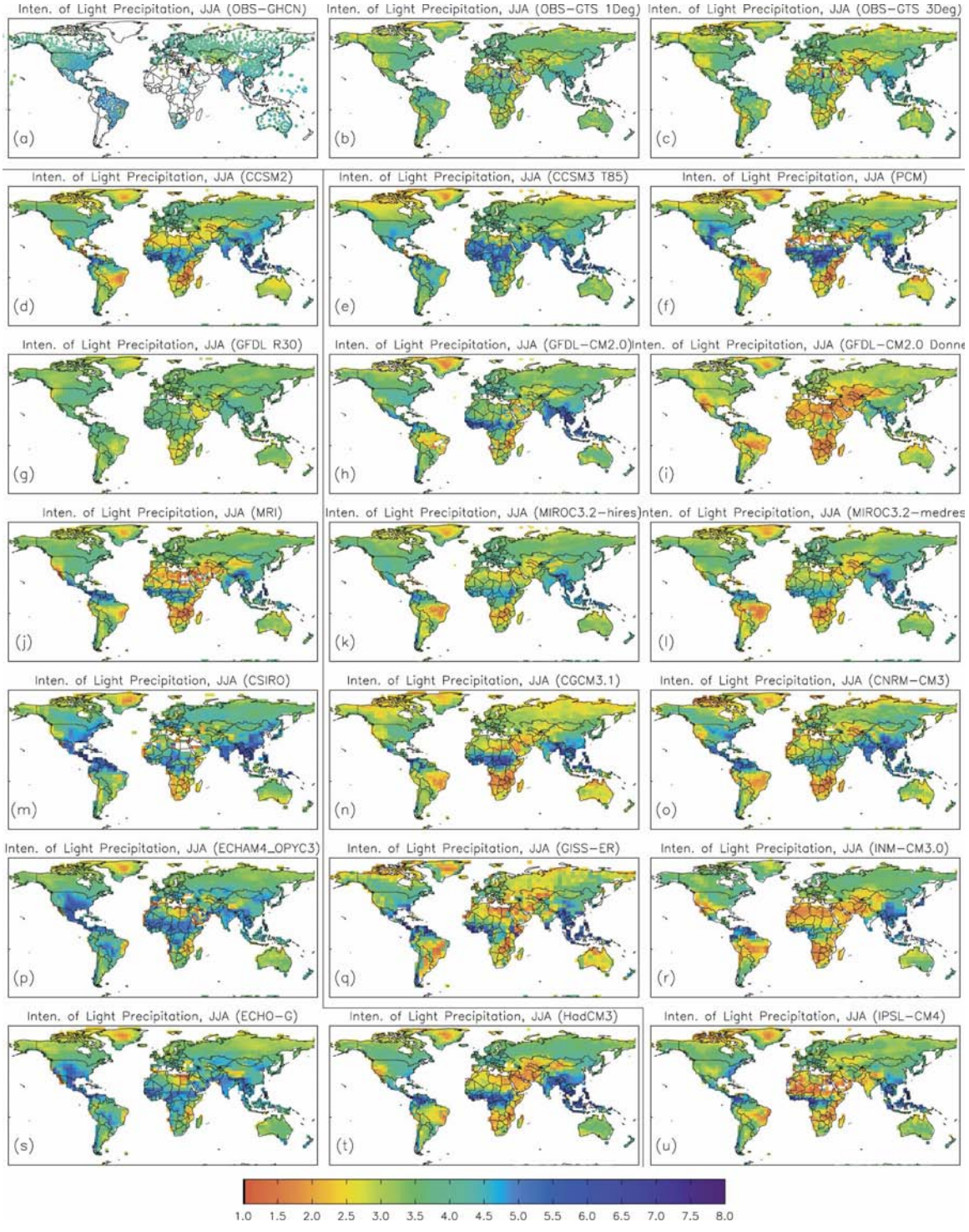

FIG. 5. Same as in Fig. 3 but for light precipitation intensity (mm day^{-1}). (a) Black colors (including open triangles and circles) indicate that light precipitation has not been observed. (b)–(u) White regions in land areas indicate that light precipitation never occurs there.

cal Africa, where summer moist convection is intense, a high precipitation intensity (>25 mm day^{-1} for OBS-GHCN and >16 mm day^{-1} for OBS-GTS) is found. In high latitudes, where the atmosphere contains less moisture, the precipitation intensity is much weaker than that at mid- and low latitudes. In dry regions, such as northern and southern Africa and the Middle East, observed precipitation never exceeds 10 mm day^{-1} (in-

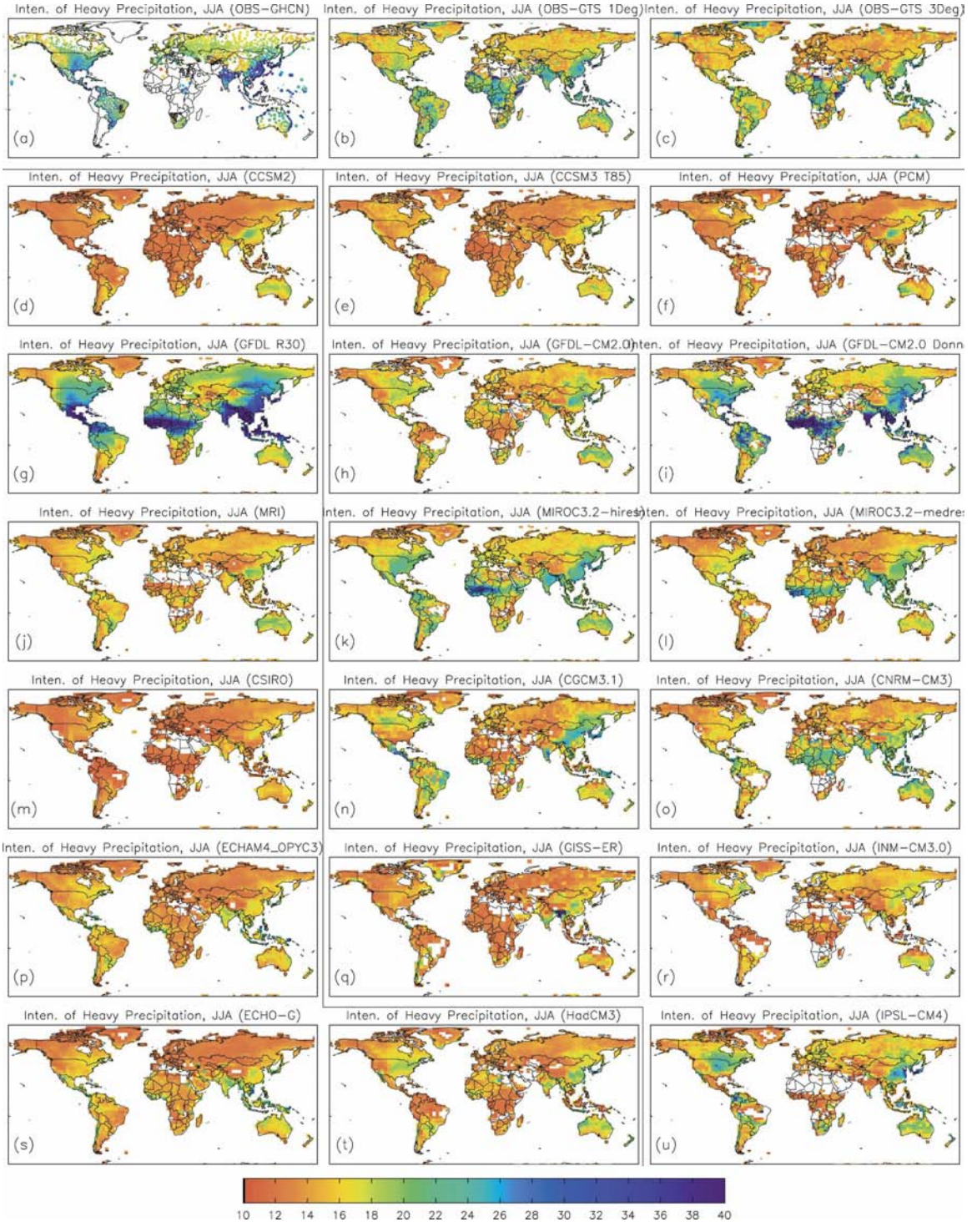

FIG. 6. Same as in Fig. 3 but for heavy precipitation intensity (mm day^{-1}).

dicated by the black open circles in Fig. 6a and the white areas in land in Figs. 6b,c).

The simulated heavy precipitation intensity shows large discrepancies from the observations for most of the models (Fig. 6). Over most of the land areas, most models underestimate the heavy precipitation intensity, especially over the mid- and low latitudes, where the simulated intensity is only ~10–15 mm day^{-1}, which is

less than half of that observed (Fig. 6). However, GFDL R30, GFDL-CM2.0 Donner, MIROC3.2 high and medium resolution are able to reproduce the high precipitation intensity over the eastern United States, tropical Africa, and the Asian monsoon regions. A few models, such as CGCM3.1 and IPSL-CM4, can simulate heavy precipitation over the eastern United States and Asia but fail over tropical Africa.

For the simulation of heavy precipitation, there are no obvious improvements in CCSM3 over CCSM2, despite the higher resolution in CCSM3. GFDL-R30 reproduces a pattern closer to observations than GFDL-CM2.0, although GFDL-R30 overestimates the heavy precipitation intensity if compared with gridded observations. The use of Donner's cumulus scheme allows the model GFDL-CM2.0 to reproduce the heavy precipitation intensity well over eastern North America, South America, and Asia. This indicates that cumulus schemes have important effects on the simulation of heavy precipitation. Both versions of MIROC3.2 show a good capability to reproduce heavy precipitation intensity over the Asian monsoon regions and tropical Africa despite the resolution differences (T106 versus T42). The high-resolution version, however, has a better simulation over the eastern United States and the Brazilian Highlands than the medium-resolution model. It can be seen that most models with a rather low resolution failed to reproduce heavy precipitation over the Brazilian Highlands.

Similarly, the models also underestimate the heavy precipitation intensity in DJF (not shown). Thus, this discrepancy is large in different seasons as well as regions.

As indicated previously, the incorrect combination of frequency and intensity has been a fairly common problem in climate models (e.g., Chen et al. 1996; Dai et al. 1999). Here we have shown that this problem is still very widespread in the CMIP2 and the newest IPCC model set. Our results further show that for light and heavy precipitation types, the models' biases are very different. For *light* precipitation, most of the models greatly *overestimate the frequency* but reproduce the observed patterns of intensity relatively well. For *heavy* precipitation, most of the models roughly reproduce the observed frequency but *underestimate the intensity*.

6. Number of days dominating total precipitation

Figure 7 shows the pattern of $\overline{N}_{67}$ as well as the anomalies observed for 1988 and 1993 over the United States. In 1988, a severe drought occurred in the central and eastern United States with very severe losses in agriculture and related industries, while in 1993 widespread flooding occurred in the central United States due to heavy rains and thunderstorms (NCDC 2004). Therefore, these two years represent two extremes of precipitation. We defined a consistent cutoff value to count the number of rainy days that accounts for the majority of total precipitation in 1988 and 1993. Similar to the calculation method of N_{67}, we first sort the daily precipitation data from the heaviest to the lightest for each year. Then we locate a cutoff rate over which 67% of annual precipitation amount occurs. The average of this cutoff rate over all the years is the mean rate that we consider as heavy rain. For 1988 and 1993, the rainy days with precipitation exceeding this mean rate were

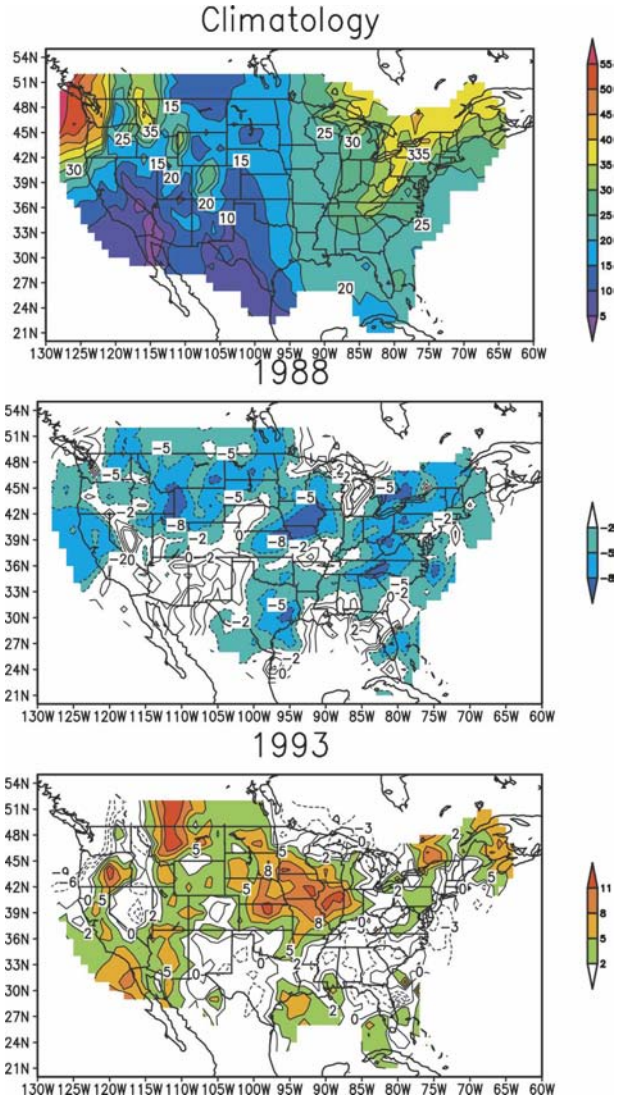

FIG. 7. The number of rainy days contributing 67% of the annual precipitation for (a) climatology (1840–2001, but with varying length for different stations), the anomalies for (b) 1988 and (c) 1993.

counted and considered as the locally determined number of major rainy days.

Figure 7a shows that 67% of the annual precipitation normally occurs within about 20–30 days in the southeast United States, 30–40 days in the Northeast, and 40–55 days in the Northwest, whereas in the dry Southwest, most of the annual precipitation typically occurs in less than 10 days. Thus, in the dry Southwest, a few missed or extra heavy rain days can have a significant impact on the climate of that year. This explains why dry regions are vulnerable to droughts.

Figures 7b,c show the impact of the number of major rainy days on the 1988 drought and 1993 floods. In 1988, much of the central United States missed 5–8 of the normal 20–30 major rainy days that occur in a normal year, contributing to the drought conditions in the Midwest and other parts of the Upper Mississippi Basin. In 1993, there were 5–11 more major rainy days over much of the central United States, making important contributions to record floods around the Mississippi River. We also note that the mean precipitation intensity for the heavy rain days in these two years is different from normal years (not shown), with generally higher intensity in the flooding regions and lower intensity in the drought regions. Further analyses show that the change in the number of major rainy days is more important than the change in the intensity in producing the drought in 1988 and the flood in 1993. An investigation on the model's simulation in these two years shows that the models are unable to reproduce the anomalous number of major rainy days in the Midwest for these two extremes of precipitation.

Figure 8 compares the long-term mean observed and simulated global distributions of the number of days contributing 67% of the total precipitation, $\overline{N}_{67}$. There are differences between $\overline{N}_{67}$ calculated using station data (Fig. 8a) and gridded data (Figs. 8b,c; e.g., over the eastern United States and Asian monsoon regions), and between 1° (Fig. 8b) and 3° grid data (Fig. 8c). Thus, this parameter is sensitive to data resolution. However, these differences are considerably smaller than those between the models and the data.

As seen in Figs. 8a–c the observations show large regional differences. For many regions in northern high latitudes, most of the annual precipitation occurs in more than 30 days (Figs. 8a–c, also see Fig. 1), and in parts of Europe the number is more than 40 days, indicating that rainfall in these regions occurs frequently but with relatively low intensity. In many regions at lower latitudes, such as the southeast United States, northern South America, and Southeast Asia, most of the annual precipitation falls in less than 30 days, indicating that precipitation there is more concentrated and intense. Figure 2 underscores that these regions are fairly wet areas with large annual precipitation amounts. In many dry regions, such as northern and southern Africa, most of Australia, the U.S. Southwest, and central Asia, most of the annual precipitation falls in relatively few days. In these areas, each locally heavy rain day is critical for annual rainfall. Thus regions where most of the annual precipitation occurs in fewer than about 10–15 days are likely to be vulnerable to droughts.

Most of the models are able to reproduce the small number of $\overline{N}_{67}$ over many dry regions, such as Australia and northern Africa (Fig. 8). However, the simulations over wet regions are poor, especially in northern South America, tropical Africa, and Indonesia, where the simulated $\overline{N}_{67}$ values exceed 160, which is 4–5 times larger than the observed. These regional biases are consistent with the precipitation frequency biases shown in Fig. 4. Similar to the frequency, the GFDL-R30, MIROC3.2 high- and medium-resolution models perform relatively well in simulating $\overline{N}_{67}$; however, the MIROC3.2 models suggest overestimates over the northern mid- and high latitudes. All of the other models substantially overestimate the number of the rainy days dominating the precipitation over most regions.

For different versions of the models, there are no large differences between CCSM2 and CCSM3, and MIROC3.2 high- and medium-resolution models, suggesting that model's resolution has only a small effect on this parameter. The GFDL-CM2.0 Donner shows some improvements over the United States compared to the GFDL-CM2.0.

A further investigation of the standard deviation of N_{67} (not shown) revealed that the largest variability is found over the arid and semiarid regions while the year-to-year variations of the N_{67} are generally small over the wet regions. This is consistent with the notion that droughts are much less likely to occur in the wet regions than in the dry areas. These data thus underscore the importance of episodes of heavy precipitation in determining the availability of water region by region.

7. Discussion

Earlier studies (Mearns et al. 1995; Chen et al. 1996; Dai et al. 1999) have indicated that a common problem in climate models is too frequent precipitation at a reduced intensity. Our investigation, based on a detailed analysis of frequency and intensity of light and heavy precipitation and N_{67}, also shows that the frequency and intensity problems still exist in the newest generation of climate models. However, this problem seems to

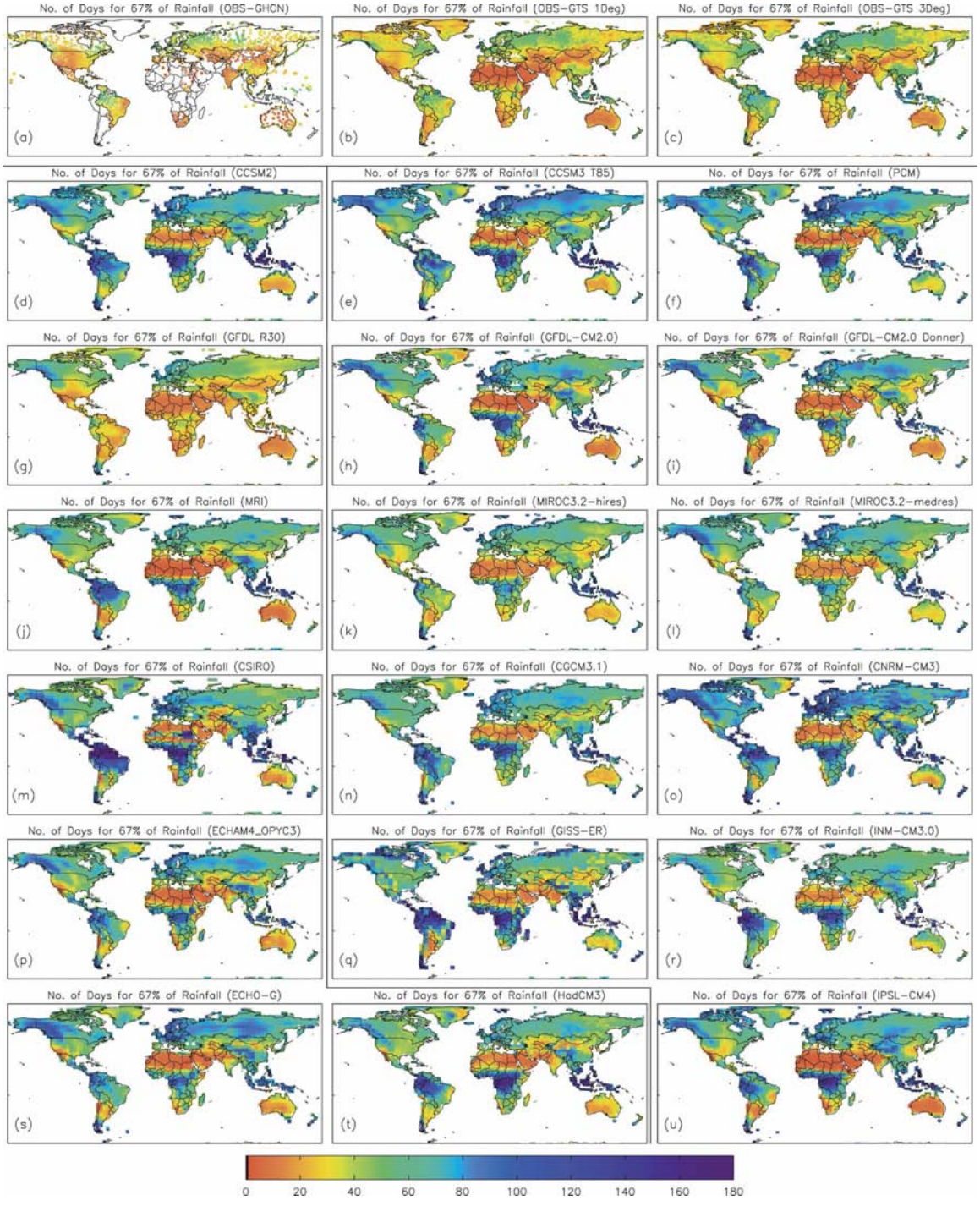

FIG. 8. Same as in Fig. 3, but for the number of rainy days contributing 67% of the annual precipitation.

be less severe in a few models such as GFDL-R30, the GFDL-CM2.0 Donner, and the MIROC3.2 high- and medium-resolution models.

The GFDL-R30 model shows a good performance in simulating the precipitation frequency and intensity and the major precipitation events. A possible reason may be related to this model's representation of heavy convective precipitation. In climate models, the total precipitation consists of convective and large-scale or stratiform precipitation. Seasonal precipitation maps (e.g., Fig. 2) show that the GFDL-R30 model is capable of simulating the observed very heavy convective pre-

cipitation over Southeast Asia and northern South America (in DJF, not shown). The GFDL-R30 model examined here uses a moist convective adjustment scheme that produces higher relative humidity and larger precipitable water than the observations (Manabe et al. 1965). In this scheme, moist convection takes place only when the lapse rate becomes superadiabatic and the relative humidity reaches 100%, whereas in the real atmosphere, moist convective condensation is usually observed when the large-scale humidity is below 100%. The biases in humidity and precipitable water associated with this scheme suggest that the GFDL-R30 model allows atmospheric convective instability/energy to accumulate before it reaches a threshold when intense convection (or convective adjustment in this model) starts (as in nature), thus avoiding the common problem in many climate models that moist convection occurs too easily and too frequently, which results in high precipitation frequency and low intensity as well as an incorrect diurnal cycle (Dai and Trenberth 2004).

The major difference between GFDL-CM2.0 and GFDL-CM2.0 Donner is that Donner's cumulus parameterization (Donner et al. 2001) was used in the latter model. Compared with the former model, the GFDL-CM2.0 Donner shows a better capability to reproduce heavy precipitation intensity. Donner's cumulus parameterization is based on mass fluxes, convective-scale vertical velocities, and mesoscale effects, while most contemporary cumulus parameterizations are based on convective mass fluxes only. Although convective cloud systems with mesoscale components account for large amounts of midlatitude rain and most tropical rain, many convection parameterizations fail to fully represent the mesoscale processes (Houze 1989). Donner et al. (2001) showed that the physical size distribution of convective systems is consistent with satellite observations only if mesoscale processes are parameterized. Ratios of stratiform-to-convective precipitation have a pattern generally similar to TRMM observations, and their magnitudes match TRMM more closely if convective vertical velocities are parameterized. This means that the use of this cumulus parameterization produces a reasonable ratio of stratiform-to-convective precipitation and is able to produce heavy precipitation. For most climate models, convection occurs too frequently and removes atmospheric moisture too efficiently, resulting in too much convective precipitation and too little stratiform precipitation (DAI).

Two versions of the MIROC3.2 provided us with a good example to investigate the effects of model resolution on the simulation of precipitation characteristics. Both models show relatively good performance in reproducing the frequency and intensity of precipitation. Although the medium-resolution model has a relatively coarse grid, there is no prominent difference for most parameters between the medium- and high-resolution models (T42 versus T106). A key component of the models' good performance could be the introduction of an empirical cumulus suppression treatment in the Arakawa–Schubert scheme, in which cumulus convection is suppressed when the cloud-mean ambient relative humidity is smaller than a certain critical value (Emori et al. 2001, 2005). In this scheme, precipitation does not always occur whenever there is large convectively available potential energy (CAPE), which is consistent with the real atmosphere. The simulated CAPE can accumulate to high values with the resulting precipitation intensity as large as that in the real world. A reasonable relationship between CAPE and daily precipitation may be a helpful diagnostic for improved simulation of precipitation characteristics in the models. However, DAI shows that the MIROC3.2, although relatively better than other models, still underestimates very heavy (>20 mm day^{-1}) precipitation, and it has a weak diurnal peak of precipitation in late afternoon, which is comparable with observed diurnal timing.

The results show that in order for models to realistically simulate the precipitation frequency and intensity, atmospheric CAPE should be allowed to accumulate so that the heavy precipitation could be produced from the intense convection. This could also improve the diurnal timing of the peak precipitation and the stratiform-to-convective precipitation ratio, for both of which the MIROC3.2 does relatively better than most other models (DAI).

Although there are many processes, such as ocean and land surface processes, large-scale atmospheric dynamics, etc., that can affect precipitation in models, the results suggest that the simulation of precipitation characteristics, especially heavy precipitation events, may be highly parameterization dependent. Improvements in moist convection schemes, especially with regards to their triggering of convection, are highly desirable for realistic simulations of precipitation frequency, intensity, and major precipitation events.

8. Summary

Precipitation characteristics are a key issue in climate research. The same amount of precipitation with different frequency and intensity could lead to different surface runoff, evaporation, and soil condition. In models it may be possible to "tune" parameters to improve amounts, but unless the amounts are right for the right

reasons—and these include the correct combination of the frequency and intensity of precipitation—it is not clear if useful forecasts or simulations will result (Trenberth et al. 2003).

In the present paper, we have analyzed land daily precipitation from individual stations and gridded observational analyses and 18 state-of-the-art fully coupled climate models to compare and evaluate model simulations of the precipitation amount, frequency, intensity, and heavy precipitation events. The observed daily precipitation reveal many interesting features, such as the small number of days that dominate the annual precipitation in many regions, and the distribution, variability, and roles of both heavy (>10 mm day^{-1}) and light precipitation (1–10 mm day^{-1}). The models examined here reproduce the broad patterns of the seasonal precipitation amounts. However, most models poorly simulate other precipitation characteristics.

For light precipitation (1–10 mm day^{-1}), most of the models simulate the observed intensity relatively well but overestimate the frequency. In contrast, for heavy precipitation (>10 mm day^{-1}), the models approximately reproduce the observed frequency patterns but underestimate the intensity. The GFDL-R30 and MIROC3.2 models tend to perform best in simulating the frequency and intensity for both light and heavy precipitation.

Consistent with the biases in precipitation frequency and intensity, we found that most of the models overestimate the annual number of the major rainy days contributing 67% of the annual precipitation over most land areas, particularly in wetter regions. The GFDL-R30 model performs best in simulating this statistic, although it also requires too many rainy days to accumulate most of the annual precipitation over Europe, Canada, Alaska, and some other regions.

The model biases in precipitation frequency and intensity found here are consistent with previous studies emphasizing that climate models generally tend to rain too frequently at reduced intensity (e.g., Dai et al. 1999; Dai and Trenberth 2004). These biases can affect surface runoff and evaporation as well as surface latent and sensible heat fluxes in the models. For example, as pointed out by Trenberth et al. (2003), light to moderate rains allow more time for water to soak into soils, thus they benefit plants and enhance subsequent surface evaporation but may result in little surface runoff and streamflow. However, intense rainfall can produce high runoff or even flash floods, but may leave subsurface soils dry. The role of these discrepancies for simulations of climate change responses (particularly insofar as water resources issues are concerned) is an important topic for research. This evaluation of model performance represents one aspect (but only one) of model evaluation.

Acknowledgments. This research was performed while the first author held a National Research Council Research Associateship Award at the NOAA/Aeronomy Laboratory. The authors are grateful to Leo Donner and Pingping Xie for providing their data and helpful suggestions. We thank Philip Duffy and an anonymous reviewer for helpful comments; Dan Cayan for constructive discussion; Leon Rotstayn, Tony Hirst, Seiji Yukimoto, Erich Roeckner, and Joerg Wegner for sharing their model information; and Jerry Meehl and Curtis Covey for their assistance in model data accesses. We acknowledge the international modeling groups for providing their data for analysis, the Program for Climate Model Diagnosis and Intercomparison (PCMDI) for collecting and archiving the model data, the JSC/CLIVAR Working Group on Coupled Modelling (WGCM) and their Coupled Model Intercomparison Project (CMIP) and the Climate Simulation Panel for organizing the model data analysis activity, and the IPCC WG1 TSU for technical support. The IPCC Data Archive at the Lawrence Livermore National Laboratory is supported by the Office of Science, U.S. Department of Energy. And thanks also go to Roy Miller and John Daniel for helpful suggestions. Author A. Dai was partially supported by the NCAR Water Cycle Across-Scales Initiative.

REFERENCES

Adler, R. F., and Coauthors, 2003: The version-2 Global Precipitation Climatology Project (GPCP) monthly precipitation analysis (1979–present). *J. Hydrometeor.,* **4,** 1147–1167.

Berry, E. X., 1967: Cloud droplet growth by collection. *J. Atmos. Sci.,* **24,** 688–701.

Betts, A. K., 1986: A new convective adjustment scheme. Part I. Observational and theoretical basis. *Quart. J. Roy. Meteor. Soc.,* **112,** 677–691.

Bony, S., and K. A. Emmanuel, 2001: A parameterization of the cloudiness associated with cumulus convection; evaluation using TOGA COARE data. *J. Atmos. Sci.,* **58,** 3158–3183.

Bougeault, P., 1985: A simple parameterization of the large-scale effects of cumulus convection. *Mon. Wea. Rev.,* **113,** 2108–2121.

Chen, M., R. E. Dickinson, X. Zeng, and A. N. Hahmann, 1996: Comparison of precipitation observed over the continental United States to that simulated by a climate model. *J. Climate,* **9,** 2223–2249.

Covey, C., K. M. AchutaRao, U. Cubasch, P. Jones, S. J. Lambert, M. E. Mann, T. J. Phillips, and K. E. Taylor, 2003: An overview of the results from the Coupled Model Intercomparison Project. *Global Planet. Change,* **37,** 103–133.

Dai, A., 2001: Global precipitation and thunderstorm frequencies. Part I: Seasonal and interannual variations. *J. Climate,* **14,** 1092–1111.

——, and K. E. Trenberth, 2004: The diurnal cycle and its depiction in the community climate system model. *J. Climate,* **17,** 930–951.

——, F. Giorgi, and K. E. Trenberth, 1999: Observed and model simulated precipitation diurnal cycles over the contiguous United States. *J. Geophys. Res.,* **104,** 6377–6402.

Del Genio, A., and M.-S. Yao, 1993: Efficient cumulus parameterization for long-term climate studies: The GISS scheme. *The Representation of Cumulus Convection in Numerical Models*, *Meteor. Monogr.*, No. 46, Amer. Meteor. Soc., 181–184.

Delworth, T. L., R. S. Stouffer, K. W. Dixon, M. J. Spelman, T. R. Knutson, A. J. Broccoli, P. J. Kushner, and R. T. Wetherald, 2002: Simulation of climate variability and change by the GFDL R30 coupled model. *Climate Dyn.,* **19,** 555–574.

——, and Coauthors, 2006: GFDL's CM2 global coupled climate models. Part I: Formulation and simulation characteristics. *J. Climate,* **19,** 643–674.

Donner, L. J., C. J. Seman, R. S. Hemiler, and S. Fan, 2001: A cumulus parameterization including mass fluxes, convective vertical velocities, and mesoscale effects: Thermodynamic and hydrological aspects in a general circulation model. *J. Climate,* **14,** 3444–3463.

Emanuel, K. A., 1991: A scheme for representing cumulus convection in large-scale models. *J. Atmos. Sci.,* **48,** 2313–2335.

Emori, S., T. Nozawa, A. Numaguti, and I. Uno, 2001: Importance of cumulus parameterization for precipitation simulation over East Asia in June. *J. Meteor. Soc. Japan,* **79,** 939–947.

——, A. Hasegawa, T. Suzuki, and K. Dairaku, 2005: Validation, parameterization dependence, and future projection of daily precipitation simulated with a high-resolution atmospheric GCM. *Geophys. Res. Lett.,* **32,** L06708, doi:10.1029/2004GL022306.

Gordon, H. B., and Coauthors, 2002: The CSIRO Mk3 Climate System Model. CSIRO Atmospheric Research Tech. Paper 60, CSIRO Atmospheric Research, Australia, 77–79.

Grandpeix, J.-Y., V. Phillips, and R. Tailleux, 2004: Improved mixing representation in Emanuel's convection scheme. *Quart. J. Roy. Meteor. Soc.,* **130,** 3207–3222.

Gregory, D., and P. R. Rowntree, 1990: A mass flux convection scheme with representation of ensemble characteristics and stability dependent closure. *Mon. Wea. Rev.,* **118,** 1483–1506.

——, R. Kershaw, and P. M. Inness, 1997: Parameterization of momentum transport by convection II: Tests in single column and general circulation models. *Quart. J. Roy. Meteor. Soc.,* **123,** 1153–1183.

Groisman, P. Ya., R. W. Knight, D. R. Easterling, T. R. Karl, G. C. Hegerl, and V. N. Razuvaev, 2005: Trends in intense precipitation in the climate record. *J. Climate,* **18,** 1326–1350.

Hack, J. J., 1994: Parameterization of moist convection in the National Center for Atmospheric Research Community Climate Model (CCM2). *J. Geophys. Res.,* **99,** 5551–5568.

Higgins, R. W., J. E. Janowiak, and Y. P. Yao, 1996: *A Gridded Hourly Precipitation Database for the United States (1963–1993).* NCEP–NCAR Climate Prediction Center Atlas No. 1, U.S. Dept. of Commerce, 47 pp.

Houze, R. A., 1989: Observed structure of mesoscale convective systems and implications for large-scale heating. *Quart. J. Roy. Meteor. Soc.,* **115,** 425–461.

Huffman, G. J., and Coauthors, 1997: The Global Precipitation Climatology Project (GPCP) combined precipitation dataset. *Bull. Amer. Meteor. Soc.,* **78,** 5–20.

Iorio, J., P. B. Duffy, M. Khairoutdinov, and D. Randall, 2004: Effect of model resolution and subgrid scale physics on daily precipitation in the continental United States. *Climate Dyn.,* **23,** 243–258.

Karl, T. R., and R. W. Knight, 1998: Secular trends of precipitation amount, frequency, and intensity in the United States. *Bull. Amer. Meteor. Soc.,* **79,** 231–241.

Lambert, S. J., and G. J. Boer, 2001: CMIP1 evaluation and intercomparison of coupled climate models. *Climate Dyn.,* **17,** 83–106.

Legates, D. R., and C. J. Willmott, 1990: Mean seasonal and spatial variability in gauge-corrected, global precipitation. *Int. J. Climatol.,* **10,** 111–127.

Le Treut, H., and Z.-X. Li, 1991: Sensitivity of an atmospheric general circulation model to prescribed SST changes: Feedback effects associated with the simulation of cloud optical properties. *Climate Dyn.,* **5,** 175–187.

Manabe, S., J. Smagorinsky, and R. F. Strickler, 1965: Simulated climatology of a general circulation model with a hydrologic cycle. *Mon. Wea. Rev.,* **93,** 769–798.

Mearns, L. O., F. Giorgi, L. McDaniel, and C. Shield, 1995: Analysis of daily variability or precipitation in a nested regional climate model: Comparison with observations and doubled CO_2 results. *Global Planet. Change,* **10,** 55–78.

Meehl, G. A., F. Zwiers, J. Evans, T. Knutson, L. Mearns, and P. Whetton, 2000: Trends in extreme weather and climate events: Issues related to modeling extremes in projections of future climate change. *Bull. Amer. Meteor. Soc.,* **81,** 427–436.

Min, S.-K., S. Legutke, A. Hense, and W.-T. Kwon, 2005: Internal variability in a 1000-year control simulation with the coupled climate model ECHO-G. Part I: Near surface temperature, precipitation, and mean sea level pressure. *Tellus*, **57A,** 605–621.

Moorthi, S., and M. J. Suarez, 1992: Relaxed Arakawa–Schubert: A parameterization of moist convection for general circulation models. *Mon. Wea. Rev.,* **120,** 978–1002.

NCDC, 2002: Data documentation for dataset 9101. NCDC Global Daily Climatology Network, version 1.0, 1–11.

——, cited 2004: Billion dollar U.S. weather disasters, 1980–2003. [Available online at http://lwf.ncdc.noaa.gov/oa/reports/billionz.html.]

Nordeng, T. E., 1994: Extended versions of the convective parameterization scheme at ECMWF and their impact on the mean and transient activity of the model in the Tropics. ECMWF Tech. Rep. 206, Reading, United Kingdom, 41 pp.

Pan, D.-M., and D. A. Randall, 1998: A cumulus parameterization with a prognostic closure. *Quart. J. Roy. Meteor. Soc.,* **124,** 949–981.

Petty, G. W., 1995: Frequencies and characteristics of global oceanic precipitation from shipboard present-weather reports. *Bull. Amer. Meteor. Soc.,* **76,** 1593–1616.

Ricard, J.-L., and J.-F. Royer, 1993: A statistical cloud scheme for use in an AGCM. *Ann. Geophys.,* **11,** 1095–1115.

Roeckner, E., and Coauthors, 1996: The atmospheric general circulation model ECHAM4: Model description and simulation of present-day climate. MPI Rep. 218, Max-Planck-Institut für Meteorologie, Hamburg, Germany, 90 pp.

Rotstayn, L. D., B. F. Ryan, and J. Katzfey, 2000: A scheme for

calculation of the liquid fraction in mixed-phase clouds in large-scale models. *Mon. Wea. Rev.,* **128,** 1070–1088.

Schmidt, G. A., and Coauthors, 2006: Present-day atmospheric simulations using GISS ModelE: Comparison to in situ, satellite, and reanalysis data. *J. Climate,* **19,** 153–192.

Shepard, D., 1968: A two dimensional interpolation function for regularly spaced data. *Proc. 23rd National Conf. of American Computing Machinery*, Princeton, NJ, 517–524.

Slingo, J. M., 1987: The development and verification of a cloud prediction scheme for the ECMWF model. *Quart. J. Roy. Meteor. Soc.,* **113,** 899–927.

Smith, R. N. B., 1990: A scheme for predicting layer clouds and their water content in a general circulation model. *Quart. J. Roy. Meteor. Soc.,* **116,** 435–460.

Sundqvist, H., 1978: A parameterization scheme for nonconvective condensation including prediction of cloud water content. *Quart. J. Roy. Meteor. Soc.,* **104,** 677–690.

——, E. Berge, and J. E. Kristjansson, 1989: Condensation and cloud parameterization studies with a mesoscale numerical weather prediction model. *Mon. Wea. Rev.,* **117,** 1641–1657.

Tiedtke, M., 1989: A comprehensive mass flux scheme for cumulus parameterization in large-scale models. *Mon. Wea. Rev.,* **117,** 1779–1800.

——, 1993: Representation of clouds in large-scale models. *Mon. Wea. Rev.,* **121,** 3040–3061.

Trenberth, K. E., A. Dai, R. M. Rasmussen, and D. B. Parsons, 2003: The changing character of precipitation. *Bull. Amer. Meteor. Soc.,* **84,** 1205–1217.

Xie, P., and P. A. Arkin, 1997: Global precipitation: A 17-year monthly analysis based on gauge observations, satellite estimates, and numerical model outputs. *Bull. Amer. Meteor. Soc.,* **78,** 2539–2558.

——, B. Rudolf, U. Schneider, and P. A. Arkin, 1996: Gauge-based monthly analysis of global land precipitation from 1971 to 1994. *J. Geophys. Res*., **101,** 19 023–19 034.

Yukimoto, S., and Coauthors, 2001: The new Meteorological Research Institute global ocean-atmosphere coupled GCM (MRI-CGCM2)—Model climate and variability. *Pap. Meteor. Geophys.,* **51,** 47–88.

Zhang, G. J., and N. A. McFarlane, 1995: Sensitivity of climate simulations to the parameterization of cumulus convection in the Canadian Climate Centre general circulation model. *Atmos.–Ocean,* **33,** 407–446.